

Linear to quadratic crossover of Cooper pair dispersion relation *

Sadhan K. Adhikari[†]

Instituto de Física Teórica, Universidade Estadual Paulista, 01405-900 São Paulo, SP, Brazil

M. Casas, A. Puente, A. Rigo

Departament de Física, Universitat de les Illes Balears, 07071 Palma de Mallorca, Spain

M. Fortes, M. A. Solís

Instituto de Física, Universidad Nacional Autónoma de México

Apdo. Postal 20-364, 01000 México, DF, Mexico

M. de Llano, Ariel A. Valladares

Instituto de Investigaciones en Materiales, Universidad Nacional Autónoma de México

Apdo. Postal 70-360, 04510 México, DF, Mexico

O. Rojo

PESTIC, Secretaría Académica & CINVESTAV, IPN, 04430 México DF, Mexico

*PACS # 64.90+b, 05.30.Fk, 05.30.Jp, 03.75.Fi. KEYWORDS Cooper pair, high- T_c superconductor

[†]corresponding author – e-mail: adhikari@ift.unesp.br, Fax: +55 11 3177 9080, address: Instituto de Física Teórica, Universidade Estadual Paulista, Rua Pamplona 145, 01405-900 São Paulo, SP, Brazil

Abstract

Cooper pairing in two (2D) and three (3D) dimensions is analyzed with a set of renormalized equations to determine its binding energy for any fermion number density and all coupling assuming a (possibly singular) pairwise residual inter-fermion interaction. Cooper pairs (CPs) with non-zero center-of-mass momentum (CMM)—usually neglected in BCS theory—are also considered and their binding energy in 2D is expanded analytically in powers of the CMM up to the quadratic term. For either 2D or 3D a Fermi-sea-dependent *linear* term in the CMM dominates the pair excitation energy in weak coupling (BCS regime) while the more familiar quadratic term prevails in strong coupling (Bose regime). The quadratic term is just the kinetic energy of the strongly-bound composite (“local”) pair in vacuum. The crossover is studied numerically and is expected to play a crucial role in a model of superconductivity as a Bose-Einstein condensation of CPs where the transition temperature is zero for all dimensionality $d \leq 2$ for quadratic but *nonzero* and very large for all $d \geq 1$ for linear dispersion. The latter range of dimensionalities is *precisely* the empirical one if quasi-1D organo-metallic superconductors are included.

PACS # 64.90+b, 05.30.Fk, 05.30.Jp, 03.75.Fi.

KEYWORDS Cooper pair, high- T_c superconductor

I. INTRODUCTION

The Cooper pair [1] (CP) problem in one dimension (1D) for an attractive delta-function inter-fermion interaction was studied [2,3], as was [4] also the corresponding Bardeen-Cooper-Schrieffer (BCS) problem [5], principally because the ground-state energy of a many-fermion system with such pair interactions can be obtained exactly [6–8] for any coupling and/or particle density. However, in two (2D) and three dimensions (3D) such a system collapses [9] to infinite binding energy per fermion and infinite particle density due to the fact that the potential well now supports an infinite number of bound states as opposed to the single one in 1D. One can work with a regularized attractive delta-function pair potential constructed [10] from square-well potentials in such a way that the resulting infinitesimally shallow well supports only *one* bound state—as in the case of the 1D delta potential. This then precludes collapse of the many-fermion system in either 2D or 3D.

These catastrophes can also be circumvented via interactions regularized in momentum space with large-momentum cutoffs [11,12]. One such regularized potential is the BCS model interaction which is of great practical use in studying Cooper pairing [1] and superconductivity [5]. Its double Fourier transform is simply $V_{pq} = -V$ (with $V \geq 0$) when $\mu - \hbar\omega_D \leq \hbar^2 p^2/2m$, $\hbar^2 q^2/2m \leq \mu + \hbar\omega_D$, and $= 0$ otherwise, where μ is the chemical potential (or Fermi surface energy for weak coupling), ω_D the Debye frequency, p and q the relative pair wavenumbers before and after interaction, and m the effective fermion mass. The BCS model interaction, however, yields critical temperatures which are too small to describe high- T_c superconductors. Although there are controversies over the precise pairing mechanism and thus over the microscopic Hamiltonian appropriate for high- T_c superconductors, some of the properties of these materials have been explained satisfactorily within a BCS-Bose crossover picture [13–33] by using a renormalized BCS theory for a short-range (possibly singular) interaction. In the weak-coupling (and/or high fermion-number density) limit of the BCS-Bose crossover one recovers the pure mean-field BCS theory of weakly-bound, severely-overlapping CPs, while for strong coupling (and/or low density) well-separated, nonoverlapping “diatomic molecular” pairs appear [13–15] in what is known as the Bose regime. For the soluble 1D model the BCS-Bose ground-state energy coincides perfectly with the exact energy at *both extremes*. In higher dimensions it is of interest to detail how renormalized Cooper pairing itself evolves *independently* of the BCS-Bose crossover picture in order to then address the possible Bose-Einstein (BE) condensation (BEC) of such pairs. We address this here in a *single-CP picture*, while considering also the important case (generally neglected in BCS theory) of non-zero center-of-mass-momentum (CMM) CPs that are expected to play a significant role in BE condensates at higher temperatures.

The BCS model interaction simulates a phonon-induced interaction which has been quite effective in explaining, e.g., the isotopic effect by using appropriate values for the cutoffs. However, high- T_c materials do not exhibit such a systematic isotopic effect normally understood in terms of the above mentioned cutoffs μ and $\hbar\omega_D$. Also, as coupling increases the chemical potential μ *decreases* in value from the (positive) Fermi energy E_F (its value at zero temperature and zero interaction), and even turns negative as the Bose regime is entered [13–15]. The Fermi surface then washes out, eliminating any physical motivation for the BCS model interaction. Alternatively, in the BCS-Bose crossover a renormalization procedure may be used to handle the large-momentum divergences [13–33]. This procedure leads to a renormalized dynamical model which may be written in terms of physical “observables” of the system (e. g., the binding

energy and scattering length of a pair of fermions in vacuum) rather than *ad hoc* cutoffs.

In this paper we derive renormalized versions of both the *t*-matrix (Lippmann-Schwinger) and Cooper equations for a pair of fermions interacting via either a zero- or a finite-range interaction, moving in the Fermi sea and in vacuum, respectively. The renormalized Cooper equation determines the CP binding energy. In 2D, Cooper binding is expressed in terms of the two-fermion binding energy in vacuum, and in 3D in terms of its scattering length. For a CP with a non-zero CMM we define a pair excitation energy as the (always positive) difference between the CP binding energy at zero and at a finite CMM. In 2D one finds an analytic expression for the CP excitation energy up to terms quadratic in the CMM which is valid for any coupling. For weak coupling only the *linear* term dominates. The linear term was mentioned as far back as 1964 [34] (see also Ref. [35]). For strong coupling, on the other hand, the *quadratic* term dominates and reduces to the kinetic energy of the strongly bound composite pair moving in vacuum. In 3D these same limiting properties hold. The transition (or crossover) from a linear to a quadratic dispersion relation for the pair excitation energy is then illustrated via numerical calculations in both 2D and 3D.

In a description of the BEC of CPs, the CP dispersion relation enters into each summand in the BE distribution function of the boson number equation from which the critical transition temperature T_c is extracted, Ref. [9] p. 40. The linear dependence on the CMM of CP binding for weak coupling leads to novel transition properties even in a heuristic BEC picture of superconductivity [36] as BE-condensing CPs. It is well-known that BEC is possible only for dimensionalities $d > 2$ for usual nonrelativistic bosons with quadratic dispersion; this limitation reappears in virtually all BEC schemes thus far applied to explain superconductivity (Refs. [28,37–40] among others). But for bosons with a *linear* dispersion relation found here in weak coupling, BEC can now occur for all $d > 1$. This is highly significant since superconductivity has been observed from 3D materials [41,42], through the quasi-2D cuprates [43,44], to the quasi-1D organo-metallics [45–47]. In contrast, BCS theory predicts $T_c > 0$ for all $d > 0$.

In Sec. II we formulate the two-body problem in vacuum for a short-range, separable interaction. In Sec. III we derive the renormalized CP equation in 2D and 3D for non-zero CMM and discuss its properties. In Sec. IV we obtain exact analytic expansions for the pair binding energy valid for any coupling in 2D up to terms quadratic in the CMM, for the delta interaction, and the effects of a finite-range interaction are briefly summarized. Finally, Sec. V offers discussion and Sec. VI conclusions.

II. TWO-BODY PROBLEM IN VACUUM

We consider fermions in a “box” with sides of length L that interact pairwise with an S-wave short-range, attractive (rank-one) separable potential in d -dimensions of the form [37]

$$V_{pq} = -(v_0/L^d)g_p g_q, \quad (1)$$

where $v_0 \geq 0$ is the interaction strength and the g_p 's are the dimensionless form factors $g_p = (1 + p^2/p_0^2)^{-1/2}$, where the parameter p_0 is the inverse range of the potential so that, e.g., $p_0 \rightarrow \infty$ implies $g_p = 1$ and corresponds to the contact or delta potential $V(r) = -v_0\delta(\mathbf{r})$. In the CP problem two fermions are assumed to interact in the momentum space above the filled Fermi sea via the effective interaction (1). The advantage of a potential of the simple form (1)

is that many relevant problems then yield analytic solutions. More realistic potentials can be approximated by a rank- N separable potential [48], and conclusions similar to the following can be generalized for such potentials.

The Lippmann-Schwinger equation for the “transition” or t -matrix with potential (1) between two fermions in free space is

$$t_{pq}(E) = V_{pq} + \sum_k V_{pk} \frac{1}{E - \hbar^2 k^2/m + i0} t_{kq}(E), \quad (2)$$

where m is the effective fermion mass and E the two-particle energy. For potential (1) the solution of Eq. (2) is given by [48]

$$t_{pq}(E) = \frac{g_p g_q}{-\frac{L^d}{v_0} - \sum_k \frac{g_k^2}{E - \hbar^2 k^2/m + i0}}. \quad (3)$$

A two-body bound state with (positive) binding energy $B_2 \geq 0$ is possible for any potential with sufficient attraction [50] and the t -matrix (3) then develops a pole at an energy $E = -B_2$, thus

$$\frac{L^d}{v_0} = \sum_k \frac{g_k^2}{B_2 + \hbar^2 k^2/m}. \quad (4)$$

In the limit $L \rightarrow \infty$ the momentum sums may be replaced by an integral

$$\sum_k \rightarrow \nu (L/2\pi)^d \int d^d k, \quad (5)$$

where d is the dimension of space, L^d the volume of the box, and ν is the number intrinsic spin degrees of freedom (usually 2 for spin up and spin down). In 1D the integral on the rhs of Eq. (4) is exact and gives the well-known binding energy $B_2 = mv_0^2/4\hbar^2$ of the single bound state, but in 2D and 3D that integral diverges for large k logarithmically and linearly, respectively. In 3D, the so-called zero-energy, on-shell t -matrix is given [49] in terms of the (S-wave) scattering length a by

$$t_{00}(0) = \frac{4\pi\hbar^2 a}{m\nu L^3}, \quad (6)$$

allowing one eventually to use a instead of v_0 ; Eq. (3) at zero energy then becomes

$$\frac{\nu}{4\pi} \frac{mL^3}{\hbar^2 a} = -\frac{L^3}{v_0} + \sum_k \frac{g_k^2}{\hbar^2 k^2/m}, \quad (3D) \quad (7)$$

where the $i0$ term in the denominator is unnecessary as the sum no longer diverges in the small k limit.

III. TWO-BODY (COOPER) PROBLEM IN FERMI SEA

The CP equation for two fermions above the Fermi surface with momenta wavevectors \mathbf{k}_1 and \mathbf{k}_2 (and finite, non-zero CMM wavevector $\mathbf{K} \equiv \mathbf{k}_1 + \mathbf{k}_2$) is given for any dimension by

$$\left[\frac{\hbar^2 k^2}{m} - E_K + \frac{\hbar^2 K^2}{4m} \right] C_k = - \sum'_q V_{kq} C_q, \quad (8)$$

where $\mathbf{k} \equiv \frac{1}{2}(\mathbf{k}_1 - \mathbf{k}_2)$ is the relative momentum wavevector, $E_K \equiv 2E_F - \Delta_K$ the total pair energy, $\Delta_K \geq 0$ the CP binding energy, $C_q \equiv \langle q | \Psi \rangle$ its wave function in momentum space, and the prime on the summation implies restriction to states *above* the Fermi surface: viz., $|\mathbf{k} \pm \mathbf{K}/2| > k_F$. For a separable interaction of the form (1) Eq. (8) can be solved for Δ_0 (analytically if $g_k = 1$) and Δ_K determined from

$$\sum'_k \frac{g_k^2}{\hbar^2 k^2/m + \Delta_K - 2E_F + \hbar^2 K^2/4m} = \frac{L^d}{v_0}, \quad (9)$$

valid also for any dimension. Although the summand in Eq. (9) is angle-independent, the restriction on the sum arising from the filled Fermi sea is a function of the relative wave vector \mathbf{k} , and therefore *angle-dependent* for $d \geq 2$. The interaction strength v_0 in Eq. (9) (which approaches zero for regularized attractive delta pair potentials [10]) may then be eliminated by combining with Eqs. (4) in 2D and (7) in 3D. Thus, in terms of the vacuum binding energy B_2 in 2D, or in terms of the vacuum scattering length a in 3D, the *renormalized CP equations* become

$$\sum_k \frac{g_k^2}{B_2 + \hbar^2 k^2/m} - \sum'_k \frac{g_k^2}{\hbar^2 k^2/m + \Delta_K - 2E_F + \hbar^2 K^2/4m} = 0 \quad (2D), \quad (10)$$

and

$$\sum_k \frac{g_k^2}{\hbar^2 k^2/m} - \sum'_k \frac{g_k^2}{\hbar^2 k^2/m + \Delta_K - 2E_F + \hbar^2 K^2/4m} = \frac{m\nu L^3}{4\pi\hbar^2} \frac{1}{a} \quad (3D). \quad (11)$$

where the primes signify, as before, the restriction $|\mathbf{k} \pm \mathbf{K}/2| > k_F$. For an attractive delta interaction $g_k = 1$ but the sums in Eqs. (4) in 2D and (7) then have large-momentum divergences. The same is true of the sums in (10) and (11). However, each of the terms on the lhs of Eq. (10) diverge in the same fashion so their difference is finite, the same holding for Eq. (11). A similar renormalization of more general scattering equations in 2D and 3D can be performed [11,12]. Also, renormalized BCS gap and number equations have been used in the BCS-Bose crossover problem [13–33]. Instead of the arbitrary cutoff usually employed in dealing with delta interactions, in Eqs. (10) and (11) we rely on physical “observables” for the sake of renormalization, viz., the ground-state binding energy B_2 in vacuum in 2D and the vacuum scattering length a in 3D. We shall work with these renormalized equations employing $0 \leq B_2 < \infty$ and $-\infty < a < +\infty$ as interaction coupling parameters in 2D and 3D, respectively, instead of the potential strength parameter $0 \leq v_0 < +\infty$ which is now eliminated.

A. Two dimensional (2D) case

The sums in Eq. (10) can be transformed to integrals using Eq. (5). However, the restriction in the second term arising from the filled Fermi sea leads to two different expressions depending on whether $\tilde{K} \equiv K/k_F$ is < 2 or > 2 , as discussed in the Appendix. For $\tilde{K} < 2$ one has

$$\int_0^{\pi/2} d\theta \left[\int_0^{\Lambda \rightarrow \infty} d\xi \frac{\xi g_\xi^2}{\tilde{B}_2 + 2\xi^2} - \int_{\xi_0(\theta)}^{\Lambda \rightarrow \infty} d\xi \frac{\xi g_\xi^2}{2\xi^2 - 2\alpha_K^2} \right] = 0, \quad \tilde{K} < 2, \quad (12)$$

where $\alpha_K^2 \equiv 1 - \tilde{\Delta}_K/2 - \tilde{K}^2/4$, $\xi_0(\theta) \equiv \sqrt{1 - \tilde{K}^2 \sin^2 \theta/4} + \tilde{K} \cos \theta/2$, with θ the angle between wavevectors \mathbf{k} and \mathbf{K} . In Eq. (12) and what follows all variables are dimensionless and are expressed either in units of the Fermi wavenumber k_F or of the Fermi energy $E_F \equiv \hbar^2 k_F^2/2m$, viz., $\tilde{B}_2 \equiv B_2/E_F$, $\xi \equiv k/k_F$, and $\tilde{\Delta}_K \equiv \Delta_K/E_F$, etc. When $\tilde{K} > 2$ the result is

$$\int_0^{\pi/2} d\theta \left[\int_0^{\Lambda \rightarrow \infty} d\xi \frac{\xi g_\xi^2}{\tilde{B}_2 + 2\xi^2} - \int_0^{\Lambda \rightarrow \infty} d\xi \frac{\xi g_\xi^2}{2\xi^2 + 2\beta_K^2} \right] + \int_0^{\theta_0} d\theta \left[\int_{\xi'_0(\theta)}^{\xi_0(\theta)} d\xi \frac{\xi g_\xi^2}{2\xi^2 + 2\beta_K^2} \right] = 0, \quad \tilde{K} > 2, \quad (13)$$

where $\beta_K^2 \equiv -\alpha_K^2$, $\xi'_0(\theta) \equiv -\sqrt{1 - \tilde{K}^2 \sin^2 \theta/4} + \tilde{K} \cos \theta/2$ and $\theta_0 = \arcsin(2/\tilde{K}) < \pi/2$. We note that the explicit normalization (5) used in transforming the sum into integral has canceled out in Eqs. (12) and (13). To deal with large-momentum divergences we have introduced a finite upper limit Λ and eventually let $\Lambda \rightarrow \infty$.

To illustrate the main physical properties of the renormalized CP equations (12) and (13) we restrict ourselves to a delta interaction, i.e., $g_\xi = 1$, as the momentum integrals in these equations can then be performed analytically. We return later to interactions of non-zero range. After some straightforward algebra the diverging terms depending on Λ in Eqs. (12) and (13) cancel out exactly, leaving

$$\int_0^{\pi/2} d\theta \ln[\xi_0^2(\theta) - \alpha_K^2] = \frac{\pi}{2} \ln\left(\frac{\tilde{B}_2}{2}\right), \quad \tilde{K} < 2, \quad (14)$$

$$\frac{\pi}{2} \ln[\beta_K^2] - \int_0^{\theta_0} d\theta \ln \frac{\xi_0^2(\theta) + \beta_K^2}{\xi_0'^2(\theta) + \beta_K^2} = \frac{\pi}{2} \ln\left(\frac{\tilde{B}_2}{2}\right), \quad \tilde{K} > 2. \quad (15)$$

Before considering the general dispersion relation relating CP energy and the finite CP CMM we examine the special case when $K = 0$. The integrands are now independent of angle. For $\tilde{K} = 0$ only Eq. (14) is of concern. In this case $\xi_0(\theta) = 1$, $\alpha_K^2 \equiv \alpha_0^2 = 1 - \tilde{\Delta}_0/2$ and we obtain the surprising identity

$$\tilde{\Delta}_0 = \tilde{B}_2, \quad (16)$$

i.e., for an attractive delta interaction the vacuum and CP binding energies for zero CMM coincide for *all* coupling, a result first obtained apparently in Ref. [29], and related to the fact that in 2D the fermionic density of states is a constant independent of E_F and thus of fermion

particle density. For a finite CMM the CP binding energies can be calculated from Eqs. (14) and (15). In Fig. 1 we plot Δ_K/E_F vs B_2/E_F for three different values of CMM, $\widetilde{K} = 0, 1,$ and 3 . The deviation from the straight line (16), i. e., the difference between B_2 and Δ_K , increases from zero with \widetilde{K} . For a non-zero \widetilde{K} a minimum threshold value of B_2/E_F is clearly required to bind a CP.

B. Three dimensional (3D) case

Similarly, in 3D Eq. (11) can be transformed into an integral using Eq. (5) and one obtains

$$\int_0^{\pi/2} d\theta \sin \theta \left[\int_0^\Lambda d\xi g_\xi^2 - \int_{\xi_0(\theta)}^\Lambda d\xi \frac{\xi^2 g_\xi^2}{\xi^2 - \alpha_K^2} \right] = \frac{\pi}{2\tilde{a}}, \quad \widetilde{K} < 2, \quad (17)$$

$$\int_0^{\pi/2} d\theta \sin \theta \left[\int_0^\Lambda d\xi g_\xi^2 - \int_0^\Lambda d\xi \frac{\xi^2 g_\xi^2}{\xi^2 + \beta_K^2} \right] + \int_0^{\theta_0} \sin \theta d\theta \int_{\xi'_0(\theta)}^{\xi_0(\theta)} d\xi \frac{\xi^2 g_\xi^2}{\xi^2 + \beta_K^2} = \frac{\pi}{2\tilde{a}}, \quad \widetilde{K} > 2, \quad (18)$$

where $\tilde{a} \equiv k_F a$ is a dimensionless scattering length. The momentum-space integrals in Eqs. (17) and (18) can be performed as in 2D for a zero-range interaction with $g_\xi = 1$. Integrating explicitly and canceling the Λ -dependent divergent terms yields

$$\int_0^{\pi/2} d\theta \sin \theta \left[\xi_0(\theta) + \frac{\alpha_K}{2} \ln \frac{\xi_0(\theta) - \alpha_K}{\xi_0(\theta) + \alpha_K} \right] = \frac{\pi}{2\tilde{a}}, \quad \widetilde{K} < 2, \quad \alpha_K^2 > 0, \quad (19)$$

$$\frac{\pi}{2}\beta_K + \int_0^{\pi/2} d\theta \sin \theta \left[\xi_0(\theta) - \beta_K \arctan \frac{\xi_0(\theta)}{\beta_K} \right] = \frac{\pi}{2\tilde{a}}, \quad \widetilde{K} < 2, \quad \alpha_K^2 < 0, \quad (20)$$

$$\frac{\pi}{2}\beta_K + \int_0^{\theta_0} d\theta \sin \theta \left[\xi_0(\theta) - \xi'_0(\theta) - \beta_K \left\{ \arctan \frac{\xi_0(\theta)}{\beta_K} - \arctan \frac{\xi'_0(\theta)}{\beta_K} \right\} \right] = \frac{\pi}{2\tilde{a}}, \quad \widetilde{K} > 2, \quad \alpha_K^2 < 0. \quad (21)$$

We note that α_K^2 may change sign in the region of integration. In order to ensure real quantities in these expressions we have separated the result into the three domains of \widetilde{K} and α_K^2 shown above.

For CPs with $\widetilde{K} = 0$ only Eqs. (19) and (20) are of concern. Again, as in 2D, since in this case $\xi_0(\theta) = 1$ and $\alpha_K^2 \equiv \alpha_0^2 \equiv -\beta_0^2 = 1 - \tilde{\Delta}_0/2$, one arrives at

$$1 + \frac{\alpha_0}{2} \ln \left| \frac{1 - \alpha_0}{1 + \alpha_0} \right| = \frac{\pi}{2\tilde{a}}, \quad \alpha_0^2 > 0, \quad (22)$$

$$\frac{\pi}{2}\beta_0 + 1 - \beta_0 \arctan \frac{1}{\beta_0} = \frac{\pi}{2\tilde{a}}, \quad \alpha_0^2 < 0. \quad (23)$$

These two equations relate the dimensionless scattering length $\tilde{a} \equiv k_F a$ in vacuum to the dimensionless CP binding energy for zero CMM $\tilde{\Delta}_0 \equiv \Delta_0/E_F$ for all coupling. In Eq. (22) the limit $\tilde{\Delta}_0 \rightarrow 0$ implies $\tilde{a} \rightarrow 0^-$ or $\tilde{a}^{-1} \rightarrow -\infty$ and corresponds to weak coupling. Alternatively, in Eq. (23) the limit $\tilde{\Delta}_0 \rightarrow \infty$ implies $\tilde{a}^{-1} \rightarrow +\infty$, or strong coupling. The transcendental equation (22) can be solved for CP binding for $\tilde{a} \equiv -|\tilde{a}| \rightarrow 0^-$. In this limit the argument of the logarithm in Eq. (22) reduces to $\tilde{\Delta}_0/8$, and one obtains

$$\tilde{\Delta}_0 \rightarrow (8/e^2) \exp(-\pi/|\tilde{a}|) \quad (\text{weak coupling}), \quad (24)$$

a result first reported by Van Hove [51]. One can also find $\tilde{\Delta}_0$ in the limit $\tilde{a} \rightarrow 0^+$, $\tilde{a}^{-1} \rightarrow +\infty$ or $\tilde{\Delta}_0 \rightarrow \infty$. Since in this limit $\beta_0 \arctan(1/\beta_0) \approx 1$, we obtain from Eq. (23)

$$\tilde{\Delta}_0 \rightarrow 2/\tilde{a}^2 \quad (\text{strong coupling}). \quad (25)$$

Equations (22) and (23) were solved numerically to obtain the exact functional dependence of $\tilde{\Delta}_0$ on $1/\tilde{a}$, and this is compared with asymptotic forms given by Eqs. (24) and (25). In Fig. 2 we plot $\tilde{\Delta}_K$ vs $1/\tilde{a}$ spanning weak to strong coupling. One sees how the asymptotic form given by Eq. (24) (short-dashed line) is close to the exact $\tilde{K} = 0$ result in weak coupling, whereas Eq. (25) (long-dashed curve) is also quite accurate over a large range for strong coupling. In the figure the CP binding for CMM $\tilde{K} = 1$ and 3 are also shown. As in 2D, CP binding in 3D with a non-zero CMM requires minimum threshold values of $(k_F a)^{-1}$.

IV. COOPER PAIR DISPERSION CURVES

A. Zero-range (delta) interactions

Eqs. (14) and (15) in 2D are valid for all CMM $K \geq 0$ and for all coupling. They can be solved numerically for the CP binding Δ_K for any CMM. However, before discussing numerical results we derive analytically the small-CMM behavior for any coupling. For small CMM only Eq. (14) is relevant. We take Eq. (14) for a small but non-zero \tilde{K} and for $\tilde{K} = 0$, and subtract one from the other. A small-CMM expansion of the resultant equation leads to the following expression *valid for any coupling* B_2/E_F in 2D

$$\varepsilon_K \equiv (\Delta_0 - \Delta_K) = \frac{2}{\pi} \hbar v_F K + \left[1 - \left\{ 2 - \left(\frac{4}{\pi} \right)^2 \right\} \frac{E_F}{B_2} \right] \frac{\hbar^2 K^2}{2(2m)} + O(K^3), \quad (2D), \quad (26)$$

where a nonnegative *CP excitation energy* ε_K has been defined, and the Fermi velocity v_F is defined through $E_F/k_F = \hbar v_F/2$. It is this excitation energy that must enter the BE distribution function in determining the critical temperature in a picture of superconductivity as a BEC of CPs [36–40]. The leading term in (26) is linear in the CMM, followed by a quadratic term. The coefficient of the quadratic term changes sign at $B_2/E_F = \Delta_0/E_F \simeq 0.379$, as one goes from weak ($B_2 = \Delta_0 \ll E_F$) to strong ($B_2 = \Delta_0 \gg E_F$) coupling. In the latter limit the quadratic term exactly becomes the kinetic energy of what was originally a CP (becoming what is sometimes called a “local pair”), viz.,

$$\lim_{\tilde{\Delta}_0 \gg 1} \varepsilon_K = \frac{\hbar^2 K^2}{2(2m)}, \quad (27)$$

the familiar nonrelativistic kinetic energy of the composite pair of mass $2m$ and CMM K in vacuum. As already mentioned, it is this dispersion relation that has been assumed in virtually all BEC studies of superconductivity (see, e.g., [28,37–40] among others). However, recent calculations in 2D and 3D of root-mean-square radii in the BCS-Bose crossover scheme when compared with experimental coherence lengths of several typical 2D cuprates [32], as well as of 3D materials [33], suggest that in either 2D or 3D one is well within the BCS (or weak-coupling) regime, and well removed from the Bose (or strong-coupling) one. This implies that the *linear* approximation to the dispersion relation would be relevant in these cases, and that perhaps a more general description of the BEC of CPs for all coupling might require the full, exact dispersion relation.

The limit given by Eq. (26) in 3D was found too complicated to be evaluated analytically, except for weak coupling. Repeating the 2D analysis without explicitly determining the coefficient of the quadratic term one gets, for weak coupling,

$$\lim_{\tilde{\Delta}_0 \ll 1} \varepsilon_K = \frac{1}{2} \hbar v_F K + O(K^2) \quad (3D), \quad (28)$$

i.e., the *same* result cited in 1964 in Ref. [34] for the BCS model interaction. We have verified that in strong coupling Eq. (27) also holds in 3D, as it should. Since the linear terms in both Eqs. (26) and (28) are identical [52] for the BCS model interaction in weak coupling, one might conjecture that the linear term *and* its coefficient is *universal* for any reasonable interaction, at least for weak coupling. This is consistent with the fact that the linear term coefficient depends *only* on properties of the Fermi sea and not on any parameters of the potential binding the CPs. In contrast, the coefficient of the quadratic term in Eq. (26) does depend on the coupling parameter B_2 .

Fig. 3 shows exact numerical results in 2D for different couplings of a dimensionless CP excitation energy ε_K/Δ_0 as function of CMM K/k_F . We note that the CPs *break up* whenever Δ_K turns negative, i.e., vanishes, or by Eq. (26) when $\varepsilon_K/\Delta_0 = 1$. These points are marked in the figure by dots. In addition to the exact results obtained by solving Eqs. (14) and (15) for typical values of B_2/E_F in weak to strong coupling, we also exhibit the results for the linear approximation [first term on the right-hand side of Eq. (26), dot-dashed lines, virtually coincident with the exact curve for $B_2/E_F \lesssim 0.1$] in weak coupling, as well as the quadratic approximation (dashed parabolas) in K/k_F as given by Eq. (27) for stronger couplings. For weak enough coupling one sees that the dispersion relation is virtually linear for the entire interval of K/k_F up to breakup. For stronger coupling the quadratic dispersion relation (27) slowly begins to dominate. The crossover from a linear to a quadratic dispersion relation manifests itself by a change in curvature from concave down to concave up—these two regions being separated by a point of inflection that moves down towards the origin as coupling is increased to infinity. The value of CMM where the point of inflection occurs is large for small values of B_2/E_F (~ 3) and gradually becomes smaller as B_2/E_F increases.

In Fig. 4 we display the 3D CP excitation energy ε_K/Δ_0 as a function of CMM K/k_F . Now, in addition to the exact results obtained by solving Eqs. (19), (20) and (21) for typical values of $1/k_F a$ spanning weak to strong coupling, we also show the results for the quadratic

approximation in K (dashed curves) as given by Eq. (27). The linear approximation Eq. (28) is valid only in the very weak-coupling limit, although an approximate linear relation holds for moderate couplings. The quadratic term starts to dominate at larger couplings, and at $1/k_F a \sim 3$ the exact solution is practically identical to the perfect quadratic relation (27).

Hence, the CP excitation energy dispersion relation will be *precisely* quadratic in both 2D and 3D only in the very strong coupling limit. In 2D this means $B_2/E_F \rightarrow \infty$, which occurs when either $B_2 \rightarrow \infty$ or when $E_F \rightarrow 0$ implying “turning off” the Fermi sea, thus recovering the vacuum *as a limit*. Similarly, $1/k_F a \rightarrow \infty$ in 3D means either strong coupling, $a \rightarrow 0$, or a vanishing Fermi sea, $k_F \rightarrow 0$.

B. Finite-range interactions

In the last subsection we studied the linear to quadratic crossover of the Cooper pair dispersion relation in 2D using the renormalized equation (12) for the (zero-range) delta interaction. For a *finite*-range interaction this crossover can be even more dramatic for strong coupling. However, we first consider this crossover in weak coupling for a finite-range interaction. In Fig. 5 we show the CP excitation energy ε_K/Δ_0 as a function of CMM K/k_F in 2D calculated with the interaction form factor $g_p = (1 + p^2/p_0^2)^{-1/2}$ with $p_0 = k_F$ (i. e., range $1/p_0$ of the order of the average fermion spacing $\sim 1/k_F$) for weak to moderate coupling, dashed curves. To compare, we also plot the zero-range result (full curves) as well as the linear relation (dot-dashed line) given by the first term on the right-hand side of Eq. (26). We find that the finite-range curves are close to the corresponding zero-range ones if they are labeled by Δ_0/E_F instead of by B_2/E_F as in Fig. 3. Hence in Fig. 5 we label the four sets of curves by their respective values of Δ_0/E_F . Although for zero-range interaction $B_2 = \Delta_0$ for all coupling, this is *not* so for finite-range interactions. The corresponding values of B_2 are given in the Figure caption. For $\Delta_0/E_F \lesssim 0.1$ the finite- and zero-range results are both almost coincident with the linear approximation but tend to separate as Δ_0/E_F increases.

For zero-range interaction the crossover in Figs. 3 and 4 is characterized by a point of inflection with positive slope. But increasing the range of interaction and its coupling the slope at the point of inflection decreases first to zero and eventually to a *negative* value. In Fig. 6 the linear to quadratic crossover in the dispersion relation for the finite-range interaction with $p_0 = k_F$ for stronger couplings is shown for 2D. In this case there is no special advantage in labeling the curves by Δ_0 , so we label them by B_2 . Results for $B_2/E_F = 3, 10$ and 20 are shown. In the zero-range case the curves gradually tend to the quadratic form as B_2 increases. For finite-range with $p_0 = k_F$, the dispersion curves develop a maximum and a minimum with a point of inflection in between. The slope at the point of inflection is now negative. Although each curve tends to quadratic forms for large K/k_F , they are quite different for small K/k_F . These minima are reminiscent of the “roton” excitation spectrum [53–55] in liquid ^4He .

V. DISCUSSION

The single-CP problem treated here may appear academic at first. However, it has serious consequences in the many-fermion problem. First we consider BEC of CPs, which could be

the fundamental mechanism of superconductivity. The familiar BEC formula for the transition temperature $T_c \simeq 3.31\hbar^2 n_B^{2/3}/m_B k_B$, with n_B the number density of bosons of mass m_B and k_B the Boltzmann constant, is a special case of the more general expression [36] for any d and any boson dispersion relation $\varepsilon_k = C_s k^s$ with $s > 0$, given by

$$T_c = \frac{C_s}{k_B} \left[\frac{s \Gamma(d/2) (2\pi)^d}{2\pi^{d/2} \Gamma(d/s) g_{d/s}(1)} n_B \right]^{s/d}. \quad (29)$$

If $\mu_B(T)$ is the boson chemical potential and $e^{\mu_B(T)/k_B T} \equiv z$ the fugacity, the Bose integrals in (29) are defined by

$$g_\sigma(z) \equiv \frac{1}{\Gamma(\sigma)} \int_0^\infty dx \frac{x^{\sigma-1}}{z^{-1}e^x - 1} = \sum_{l=1}^\infty \frac{z^l}{l^\sigma} \xrightarrow{z \rightarrow 1} \zeta(\sigma), \quad (30)$$

the last identification holding when $\sigma > 1$, where $\zeta(\sigma)$ is the Riemann Zeta-function of order σ . The function $\zeta(\sigma) < \infty$ for $\sigma > 1$, while the series $g_\sigma(1)$ diverges for all $\sigma \leq 1$. For $s = 2$, $C_s = \hbar^2/2m_B$ and in 3D $\zeta(3/2) \simeq 2.612$; this leads to the familiar T_c -equation cited above. Since $g_{d/2}(1)$ diverges for all $d/2 \leq 1$, we have that $T_c = 0$ for all $d \leq 2$. But for the *linear* dispersion case $s = 1$, from (26) and (28) one has $C_s = a(d)\hbar v_F$ where $a(d) \equiv 2/\pi$ and $1/2$ in 2D and 3D, respectively. Consequently, one has another special case of (29) which is

$$T_c = \frac{a(d)\hbar v_F}{k_B} \left[\frac{\pi^{(d+1)/2} n_B}{\Gamma[(d+1)/2] g_d(1)} \right]^{1/d}. \quad (31)$$

Now $T_c = 0$ for all $d \leq 1$ only, or $T_c > 0$ for all $d > 1$: this is precisely the range of dimensionalities for all known superconductors if one includes the quasi-1D organo-metallic Bechgaard salts [45–47].

The above holds for “unbreakable” CPs, i.e., bosons existing for all CMM so that the integrals over momenta go from 0 to ∞ . However, we have seen (e.g., in Fig. 3) that CPs can break up above a certain CMM K_0 , which increases in value as coupling is increased and tends to infinity in infinite coupling. But in very weak coupling the CP breakup K_0 is defined by $\Delta_{K_0} = 0$, or by $\varepsilon_{K_0}/\Delta_0 \equiv (\Delta_0 - \Delta_{K_0})/\Delta_0 = 1$. From Eqs. (26) or (28) in 2D and 3D, respectively, this condition gives $K_0 \simeq \Delta_0/a(d)\hbar v_F \rightarrow 0$ as $\Delta_0 \rightarrow 0$. The total number of such CPs is then

$$N = N_0(T) + \sum_{K \neq 0}^{K_0} \left[e^{\{\varepsilon_K - \mu_B(T)\}/k_B T} - 1 \right]^{-1}, \quad (32)$$

where $N_0(T)$ is the number of CPs in the $K = 0$ state. At $T = T_c$ both $N_0(T_c)$ and $\mu_B(T_c)$ virtually vanish so that using (5) with $\nu = 1$ (32) then gives

$$T_c \simeq \frac{n_B(d-1)[2\pi a(d)\hbar v_F]^d}{B_d k_B \Delta_0^{d-1}} \xrightarrow{\Delta_0 \rightarrow 0} \infty, \quad (33)$$

where $B_d = 2\pi$ or $4\pi/3$ in 2D or 3D, respectively. Hence, since in the above limit all CPs are condensed in the zero momentum state at all temperatures the critical temperature T_c

must be *infinite*. Consequently, for intermediate coupling in 2D one expects a finite T_c lying somewhere between the two above extremes, zero and infinity. In order to calculate this finite T_c for the many-body system at an intermediate coupling one must introduce the appropriate breakup K_0 of the CMM and the CP dispersion relation in Eq. (32) and evaluate the sum by setting $N_0(T_c) \simeq \mu_B(T_c) \simeq 0$ to determine T_c in the usual fashion. Detailed calculations of this finite T_c using the BCS model interaction yielded a value which is still almost an order of magnitude too large [57] compared with the empirical range of $T_c \approx (0.01 - 0.06)T_F$ [58–60] for cuprates—even for a moderate coupling of $\lambda \equiv N(0)V = 1/2$ where $N(0)$ is the density of states at the Fermi surface and V the attractive coupling constant of BCS model interaction. Furthermore, the calculated T_c is almost 20 times larger than that of the BCS theory using the same model interaction at the same coupling value. Significantly, T_c is *no longer* zero as would be predicted in a BEC picture by a quadratic relation appropriate for CPs in vacuum—a result that suggested to many that BEC is irrelevant for quasi-2D cuprate superconductors. Elaborate calculations must still be performed with the full, exact CP dispersion relation in order to find a more accurate BEC T_c for this many-body system, including refinements such as allowing for *unpaired fermions* (created by both temperature and coupling breakup effects) that coexist with the (breakable) CPs in a more realistic binary boson-fermion mixture model.

We next address the interesting question whether the CP linear dispersion is maintained in the many-body excitation spectrum as one reduces the coupling to zero. The single CP problem is probably intimately connected with many-body (collective) excitations (or modes), some of which also display a linear (sound-like) dispersion relation. Collective modes in a superconductor have been discussed since the late 1950’s by several workers; a review of the early 3D work by Martin is available [61], as is a more recent treatment including 2D by Belkhir and Randeria [62]. We are currently studying this possible connection in terms of the Bethe-Salpeter equation for hole-hole (hh), particle-hole (ph) as well as the particle-particle (pp) CPs considered in this paper. What has emerged so far is that with a many-CP BCS ground state the linear dispersion does *not* survive as one reduces coupling towards zero for either pp or hh CPs, but does survive for the ph (sometimes called the Anderson-Bogoliubov-Higgs) mode of excitation energy $\hbar v_F K / \sqrt{d}$ for $d = 2$ or 3 in the zero coupling limit. However, the BCS ground state does not emerge until *at and below a much smaller critical temperature* than the BEC one. Furthermore, the linear dispersion *is* maintained for both pp and hh CPs with an ideal Fermi gas ground state, making this linearity very likely to play a nontrivial role at those higher BEC T_c ’s.

Finally, our CPs are taken as “bosonic” even though they do *not* obey (Ref. [34] p. 38) Bose commutation relations. This is because for a given K they have *indefinite* occupation number since for fixed K there are (in the thermodynamic limit) an indefinitely large number of allowed (relative wavenumber) k values, so that—for any coupling and thus any degree of overlap between them—CPs do in fact obey the Bose-Einstein distribution from which BEC is determined.

VI. CONCLUSIONS

The single CP problem with non-zero CMM is studied in 2D and 3D as it evolves (or *crosses over*) by varying the interfermion short-range pair interaction from weak to strong.

The CP excitation energy is exhibited as a function of its CMM. For weak coupling, the correct excitation energy is a *linear* dispersion relation in the CMM, and changes gradually to a *quadratic* relation as coupling increases. For a zero-range pair interaction in the curve for the dispersion relation one typically has a point of inflection with a positive slope separating a region of concave-down curvature for small CMM from a region of concave-up curvature for large CMM. For finite-range pair interactions of sufficiently long range, the slope at the point of inflection changes from positive to zero and eventually becomes negative. This leads to maxima and “roton-like” minima in the CP dispersion curves. These results will play a critical role in a model of superconductivity based on BE condensation of CPs as they yield, even in 2D, nonzero BEC transition temperatures that interpolate between very large values in weak coupling down to the expected 2D zero T_c value in strong. Lastly, although our study is based on a separable form of the interactions we expect our conclusions on the CP dispersion relation to be valid more generally, and applicable to both superconductivity and superfluidity. As to the latter, e.g., a longstanding conjecture on how liquid helium-3, as an assembly of neutral fermions for which the two-body scattering length is measurable, becomes superfluid in the millikelvin region is precisely in terms of CPs formed from some of the original fermions, which in turn suffer a BEC – supplemented, of course, by later adding the effects of interactions. This conjecture may be testable experimentally in the near future [63].

VII. APPENDIX

The restriction that both particles lie above the Fermi sea in Eq. (10) can be written as

$$(\mathbf{k}/k_F \pm \mathbf{K}/2k_F)^2 - 1 = \xi^2 \pm \xi \widetilde{K} \cos \theta + \widetilde{K}^2/4 - 1 \geq 0, \quad (\text{A. 1})$$

where $\xi \equiv k/k_F$ and $\widetilde{K} \equiv K/k_F$. The equality leads to two pairs of roots in ξ , say $\xi_{1,2} = -a \pm b$ and $\xi_{3,4} = a \pm b$, where $a \equiv (\widetilde{K}/2) \cos \theta$, $b \equiv \sqrt{1 - (\widetilde{K}^2/4) \sin^2 \theta}$, and θ the angle between \mathbf{k} and \mathbf{K} .

For $\widetilde{K} < 2$, $b > a$, one root of the two pairs is positive and the other negative. Thus, Eq. (A. 1) can be satisfied provided that $\xi > \xi_1, \xi_2, \xi_3, \xi_4$, or specifically, if $\xi > \xi_0(\theta) \equiv a + b$.

For $\widetilde{K} > 2$ and $\theta > \theta_0 \equiv \arcsin(2/\widetilde{K})$, b becomes imaginary and Eq. (A. 1) is satisfied for all ξ . Therefore, there is no restriction in the integration over ξ . However, for $\widetilde{K} > 2$ and $\theta < \theta_0$, $b < a$ the pair of roots $\xi_{1,2}$ are both negative while the pair $\xi_{3,4}$ are both positive (with $\xi_3 > \xi_4$). Consequently, in both cases Eq. (A. 1) is satisfied only if ξ is in the interval $[0, \xi'_0(\theta) \equiv a - b]$, and in the interval $[\xi_0(\theta), \infty]$, respectively. Using these restrictions on the ξ integration in Eq. (10) one arrives at Eqs. (12) and (13). Similar arguments apply in 3D.

Acknowledgments: M.deLl. thanks S. Fujita for discussions, D.M. Eagles for reading the manuscript, and V.V. Tolmachev for extensive correspondence. Partial support from UNAM-DGAPA-PAPIIT (México) # IN102198, CONACyT (México) # 27828 E, DGES (Spain) # PB95-0492 and FAPESP (Brazil) is gratefully acknowledged.

REFERENCES

- [1] L. N. Cooper, Phys. Rev. 104 (1956) 1189.
- [2] M. Casas, C. Esebbag, A. Extremera, J. M. Getino, M. de Llano, A. Plastino, and H. Rubio, Phys. Rev. A 44 (1991) 4915.
- [3] V. C. Aguilera-Navarro, M. de Llano and M. A. Solís, Eur. J. Phys. 20 (1999) 177.
- [4] R. M. Quick, C. Esebbag and M. de Llano, Phys. Rev. B 47 (1993) 11512.
- [5] J. Bardeen, L. N. Cooper and J. R. Schrieffer, Phys. Rev. 108 (1957) 1175.
- [6] J. B. McGuire, J. Math. Phys. 5 (1964) 4915.
- [7] M. Gaudin, Phys. Lett. A 24(1967) 55.
- [8] C. N. Yang, Phys. Rev. 168 (1968) 1920.
- [9] A. L. Fetter and J. D. Walecka, *Quantum Theory of Many-Particle Systems* (McGraw-Hill, NY, 1971) p. 31.
- [10] P. Gosdzinsky and R. Tarrach, Am. J. Phys. 59 (1991) 70.
- [11] S. K. Adhikari and A. Ghosh, J. Phys. A 30 (1997) 6553.
- [12] S. K. Adhikari, T. Frederico, Phys. Rev. Lett. 74 (1995) 4572.
- [13] A. J. Leggett, J. Phys. (Paris) Colloq. 41 (1980) C7-19.
- [14] K. Miyake, Prog. Theor. Phys. 69 (1983) 1794.
- [15] M. Randeria, J. -M. Duan, and L. -Y. Shieh, Phys. Rev. B 41 (1990) 327.
- [16] J. Labbé, S. Barisić, and J. Friedel, Phys. Rev. Lett. 19 (1967) 1039.
- [17] D. M. Eagles, Phys. Rev. 186 (1969) 456.
- [18] R. Micnas, J. Ranninger, and S. Robaszkiewicz, Rev. Mod. Phys. 62 (1990) 113.
- [19] D. van der Marel, Physica C 165, 35 (1990); M. Drechsler and W. Zwirger, Ann. der Physik 1 (1992) 15.
- [20] A. S. Alexandrov and N. F. Mott, Rep. Prog. Phys. 57 (1994) 1197.
- [21] J. E. Hirsch, Physica C 179 (1991) 317.
- [22] A. Tokumitsu, K. Miyake, and K. Yamada, Phys. Rev. B 47 (1994) 11988.
- [23] D. Dzhumanov, P. J. Maimatov, A. A. Baratov, and N. I. Rahmatov, Physica C 235-240 (1994) 2339.
- [24] F. Pistolesi and G. C. Strinati, Phys. Rev. B 53 (1996) 15168.
- [25] J. Ranninger, and also M. Randeria, in *Bose-Einstein Condensation*, Eds. A. Griffin, D. Snoke, and S. Stringari, (Cambridge University Press, Cambridge, 1995).
- [26] E. V. Gorbar, V. M. Loktev, and S. G. Sharapov, Physica C 257 (1996) 355.
- [27] Q. Chen, I. Kosztin, B. Jankó, and K. Levin, Phys. Rev. B 59 (1999) 7083.
- [28] R. Haussmann, Phys. Rev. B 49 (1994) 12975.
- [29] S. K. Adhikari and A. Ghosh, Phys. Rev. B 55 (1997) 1110.
- [30] A. Ghosh and S. K. Adhikari, Eur. Phys. J. B 2 (1998) 31.
- [31] A. Ghosh and S. K. Adhikari, J. Phys.: Cond. Matter 10 (1998) 135.
- [32] M. Casas, J. M. Getino, M. de Llano, A. Puente, R. M. Quick, H. Rubio, and D. M. van der Walt, Phys. Rev. B 50 (1994) 15945.
- [33] R. M. Carter, M. Casas, J. M. Getino, M. de Llano, A. Puente, H. Rubio, and D. M. van der Walt, Phys. Rev. B 52 (1995) 16149.
- [34] J. R. Schrieffer, *Theory of Superconductivity* (Benjamin, Reading, MA, 1964) p. 33.
- [35] S. Fujita and S. Godoy, *Quantum Statistical Theory of Superconductivity* (Plenum, NY, 1996).

- [36] M. Casas, A. Rigo, M. de Llano, O. Rojo, and M. A. Solís, *Phys. Lett. A* 245 (1998) 55.
- [37] P. Nozières and S. Schmitt-Rink, *J. Low. Temp. Phys.* 59 (1985) 195.
- [38] V. V. Tolmachev, submitted for publication to *Phys. Lett. A*
- [39] R. Friedberg and T. D. Lee, *Phys. Rev. B* 40 (1989) 6745.
- [40] J. M. Blatt, *Theory of Superconductivity* (Academic, NY, 1964) esp. p. 94, and refs. therein).
- [41] A. F. Hebard, M. J. Rosseinsky, R. C. Haddon, D. W. Murphy, S. H. Glarum, T. T. M. Palstra, A. P. Ramirez, and A. R. Kortan, *Nature* 350 (1991) 600.
- [42] A. P. Ramirez, *Superconductivity Rev.* 1 (1994) 1.
- [43] H. Ding, *Nature* 382 (1996) 51.
- [44] D. J. Scalapino, *Phys. Rep.* 250 (1995) 329.
- [45] D. Jérôme, *Science* 252 (1991) 1509.
- [46] J. M. Williams, A. J. Schultz, U. Geiser, K. D. Carlson, A. M. Kini, H. H. Wang, and W. K. Kwok, M. H. Whangbo, and J. E. Schirber, *Science* 252 (1991) 1501.
- [47] H. Hori, *Int. J. Mod. Phys. B* 8 (1994) 1.
- [48] S. K. Adhikari, *Variational Principles and the Numerical Solution of Scattering Problems* (Wiley, NY, 1998).
- [49] P. Roman, *Advanced Quantum Theory* (Addison-Wesley, NY, 1965) p. 175; Ref. [48] p. 42.
- [50] S. K. Adhikari and T. Frederico, *Eur. Phys. J. B* 5 (1998) 219.
- [51] L. Van Hove, *Physica* 25 (1959) 849.
- [52] M. Casas, S. Fujita, M. de Llano, A. Puente, A. Rigo, M. A. Solís, *Physica C* 295 (1998) 93.
- [53] L. D. Landau, *J. Phys. USSR*, 11 (1947) 91.
- [54] R. P. Feynman, *Phys. Rev.* 91 (1953) 1301.
- [55] R. P. Feynman 94 (1954) 262.
- [56] M. Casas, A. Puente, A. Rigo, N. J. Davidson, R. M. Quick, M. Fortes, M. A. Solís, M. de Llano, O. Navarro, A. A. Valladares and O. Rojo, *Proc. of II Int. Conf. New Theories, Discoveries, and Applications of Superconductors and Related Materials* (Las Vegas, 1999) *Int. J. Mod. Phys. B* (in press).
- [57] M. Casas, A. Puente, A. Rigo, N. J. Davidson, R. M. Quick, M. Fortes, M. A. Solís, M. de Llano, O. Navarro, A. A. Valladares and O. Rojo, *Proc. of II Int. Conf. New Theories, Discoveries, and Applications of Superconductors and Related Materials* (Las Vegas, 1999); *Int. J. Mod. Phys. B* (in press).
- [58] Y. J. Uemura, L. P. Le, G. M. Luke, B. J. Sternlieb, W. D. Wu, J. H. Brewer, T. M. Riseman, C. L. Seaman, M. B. Maple, M. Ishikawa, D. G. Hinks, J. D. Jorgensen, G. Saito, H. Yamochi, *Phys. Rev. Lett.* 66 (1991) 2665.
- [59] Y. J. Uemura, A. Keren, L. P. Le, G. M. Luke, B. J. Sternlieb, W. D. Wu, J. H. Brewer, R. L. Whetten, S. M. Huang, S. Lin, R. B. Kaner, F. Diederich, S. Donovan, G. Gruner, and K. Holczer, *Nature* 352 (1991) 605.
- [60] Y. J. Uemura and G. M. Luke, *Physica B* 186-188 (1993) 223.
- [61] P. C. Martin, in *Superconductivity* (ed. by R. D. Parks) Vol. 1 (Marcel Dekker, 1969).
- [62] L. Belkhir and M. Randeria, *Phys. Rev. B* 49 (1994) 6829.
- [63] B. Levi, *Phys. Today*, Oct. 1999, p. 17.

VIII. FIGURE CAPTIONS

1. Dimensionless CP binding energy Δ_K/E_F in 2D, calculated numerically from Eqs. (14) and (15), for vanishing and non-zero CMM wavenumber K , *vs* different couplings (i.e., dimensionless two-body binding energies in vacuum B_2/E_F) for $K/k_F = 0, 1$ and 3 . The curves are labeled by the respective values of two-body binding energy in vacuum K/k_F .

2. Same as in Fig. 1 but in 3D, calculated from Eqs. (19), (20) and (21), except that coupling is now measured by the inverse dimensionless scattering length $1/k_F a$. Long-dashed quadratic curve (25) is valid for strong coupling while short-dashed straight line (24) holds for weak coupling.

3. Dimensionless CP excitation energy ε_K/Δ_0 *vs* K/k_F in 2D, calculated from Eqs. (14) and (15) for different couplings B_2/E_F , full curves. The dot-dashed line is the linear approximation (virtually coincident with the exact curve for B_2/E_F as small as 0.1) while the dashed curve is the quadratic term of Eq. (27). Dots denote values of CMM wavenumber where the CP breaks up, i.e., where Δ_K turns negative.

4. Same as Fig. 3 in 3D calculated from Eqs. (19), (20) and (21) except that coupling is measured by the dimensionless inverse scattering length $1/k_F a$. Dashed curves are the quadratic term of Eq. (27). Dots denote the respective breakup CMM values for the CPs, as explained in Fig. 3.

5. Dimensionless CP excitation energy ε_K/Δ_0 *vs* K/k_F in 2D for different couplings expressed as Δ_0/E_F . The dot-dashed line is the linear approximation; the dashed curve is the result for the finite-range interaction $p_0 = k_F$, and the full curve is the zero-range result. For the finite-range potential $\Delta_0/E_F = 0.1, 0.5, 1.0$ and 2.0 correspond to $B_2/E_F = 0.469, 1.4, 2.45$ and 4 , respectively. Dots and squares mark values of CMM wavenumber where the CP breaks up, as explained in Fig. 3. The curves are labeled by the respective values of Δ_0/E_F .

6. Dimensionless CP excitation energy ε_K/Δ_0 *vs* K/k_F in 2D for different couplings B_2/E_F . The full curve is the exact zero-range result; the short-dashed one the quadratic approximation; the long-dashed one the exact finite-range result with $p_0 = k_F$. Each set of three curves is labeled by their dimensionless two-body binding energy in vacuum B_2/E_F .

Fig. 1

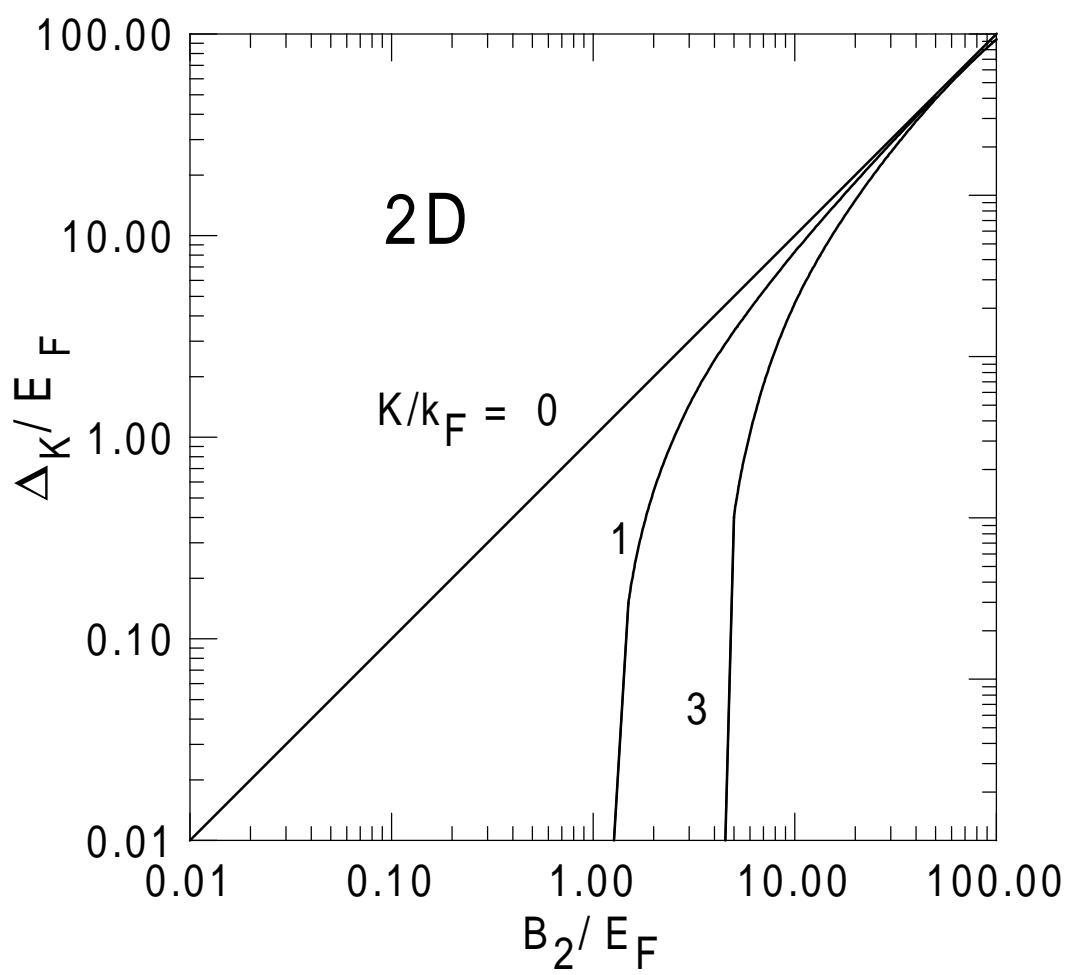


Fig. 2

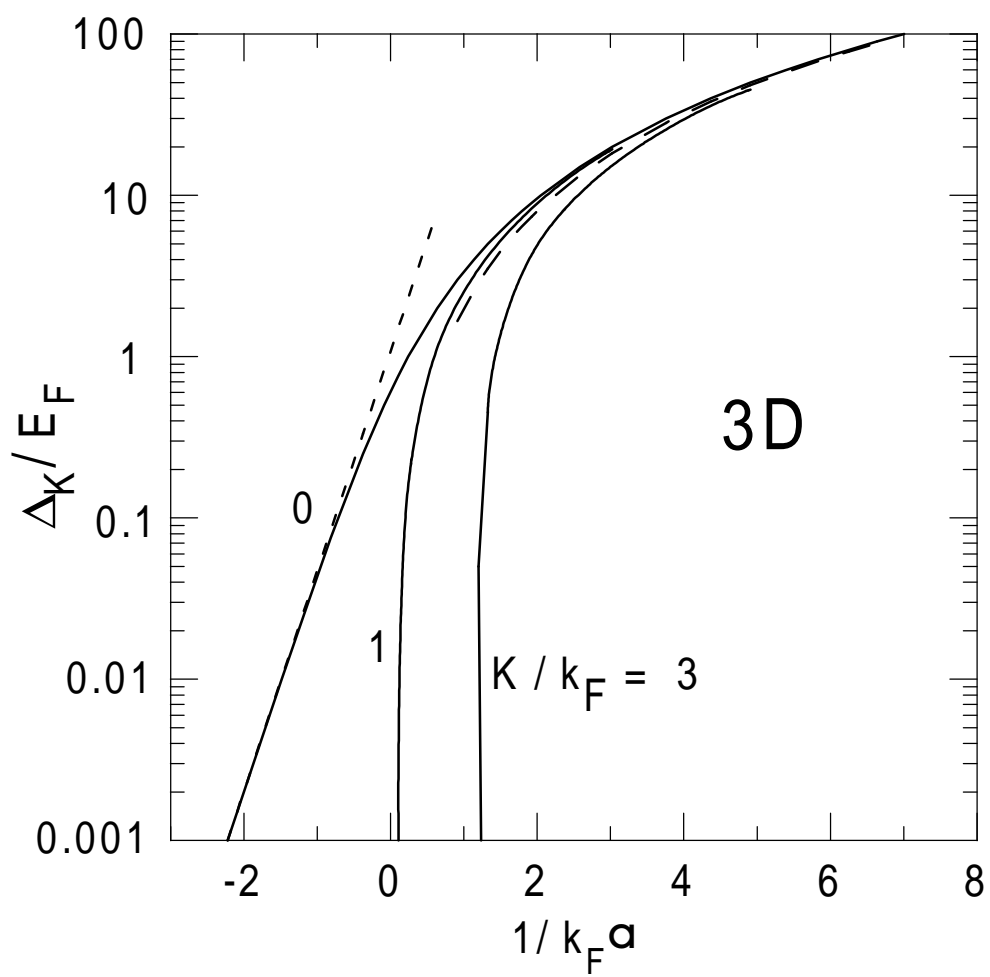


Fig. 3

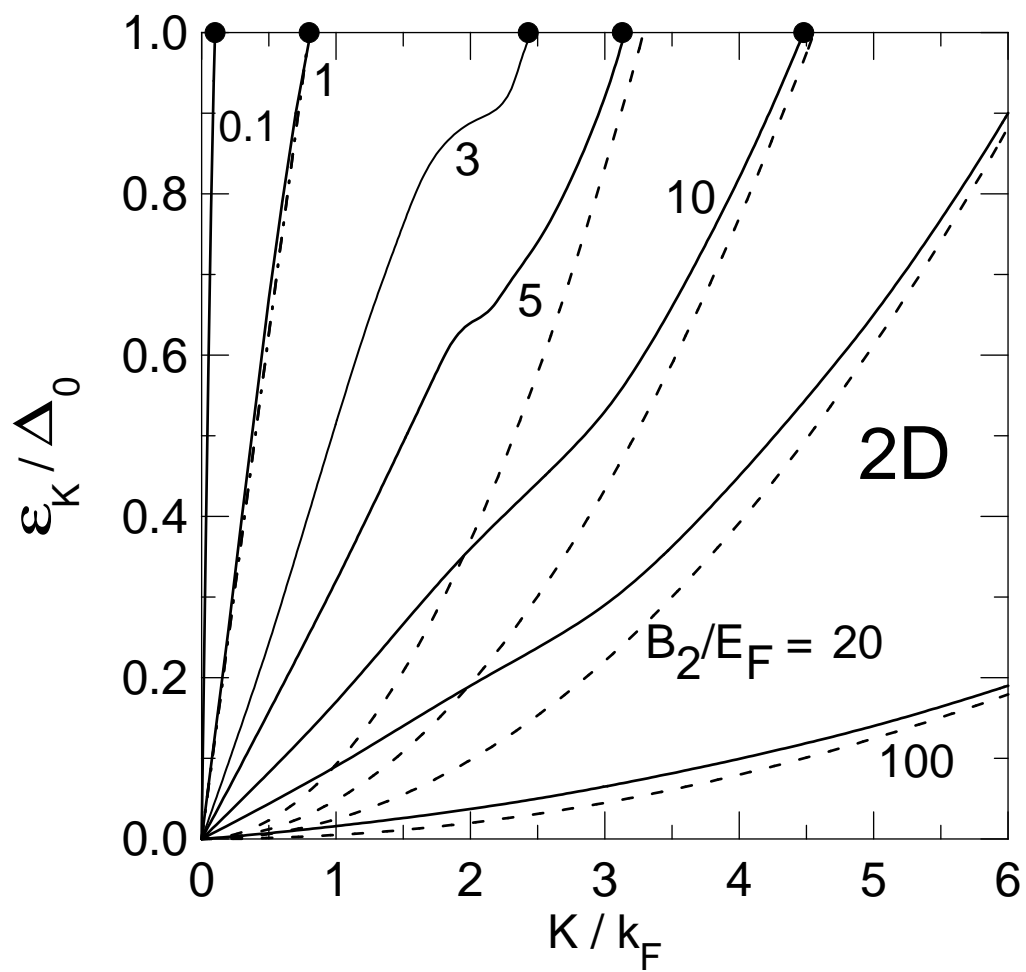


Fig. 4

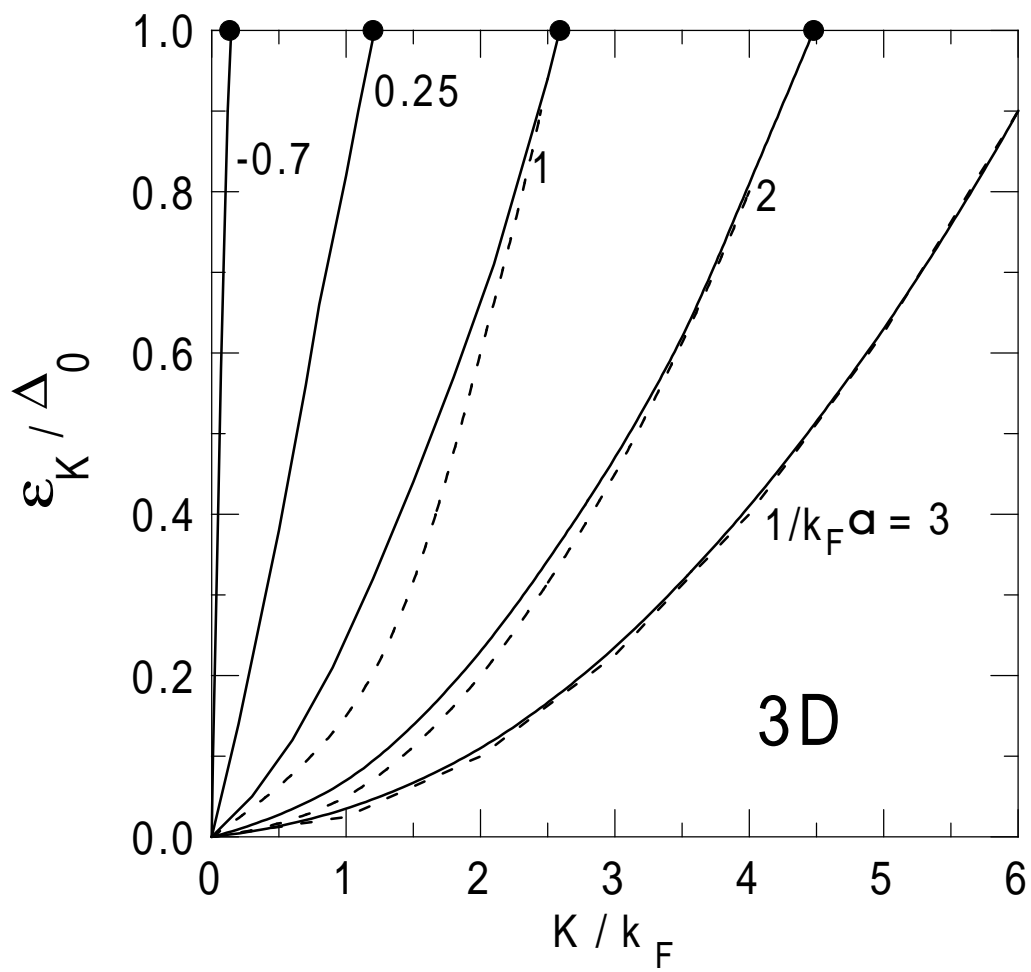


Fig. 5

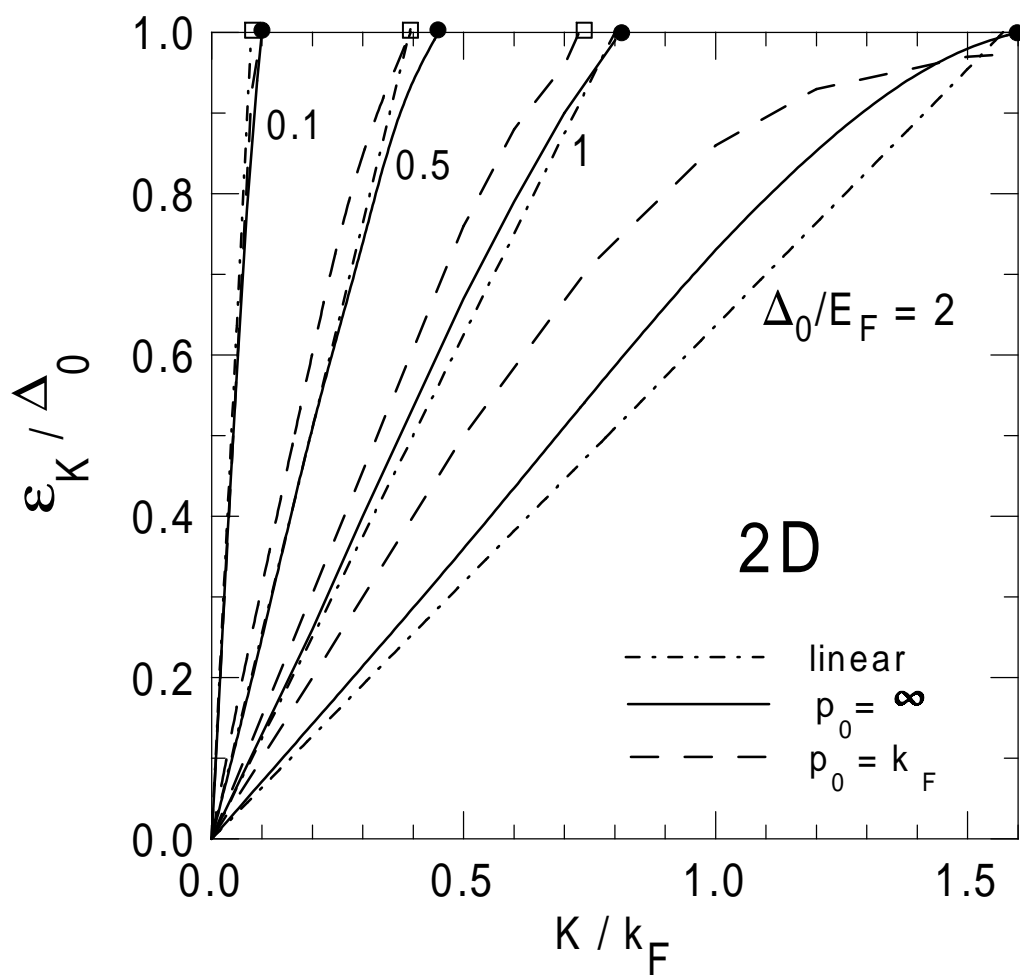


Fig. 6

